MICROSTRUCTURAL ASPECTS OF CAST Fe-Cr-Mo-C ALLOY

WIECZERZAK Krzysztof[1*], BAŁA Piotr[1,2], STĘPIEŃ Milena[2], CIOS Grzegorz[2], KOZIEŁ Tomasz[1]

AGH University of Science and Technology,

[1]Faculty of Metals Engineering and Industrial Computer Science,

[2]Academic Centre for Materials and Nanotechnology,

Al. A. Mickiewicza 30, 30-059 Krakow, Poland, EU

**Corresponding author, e-mail: kwiecz@agh.edu.pl*

Abstract

Fe-25Cr-5Mo-0.82C alloy was synthesized in an arc furnace in high purity argon atmosphere and crystallized on water-cooled copper mould. The cross section of the ingot was examined by light microscopy, scanning electron microscopy (SEM), X-ray diffraction (XRD) and its Vickers hardness determined. The microstructure is composed of primary and secondary dendrites Fe-Cr-Mo solid solution with equiaxed and elongated morphology, depending on the nature of the crystallization. In the interdendritic regions complex $M_{23}C_6$ carbides are present. The average hardness of the alloy is 264±5 HV10.

Keywords: Fe-Cr-Mo-C alloy, cast alloy, carbides, SEM, XRD

1. INTRODUCTION

In Fe-Cr-C alloys, produced with conventional techniques, it is possible to obtain microstructures composed of α-ferrite and complex carbides such as M_3C, M_7C_3 and $M_{23}C_6$ [1÷3]. The formation of the various types of carbides depends on the chemical composition of the alloy [4,5]. Alloys from Fe-Cr-C system are used as tool steels and hardfacing materials [6-10]. It should be mentioned that complex chromium carbides are also commonly used as a strengthening phase in nickel based superalloys and cobalt based alloys (Stellites), in many cases being present in association with the MC carbides (M = Nb, Zr, Ta, Hf) [11-20].

Molybdenum in Fe-Mo-C alloys can form MoC, MC and complex-type carbides such as $M_{23}C_6$ or M_6C [3,21÷23]. According to Palcut et al. [24] in low alloyed steels molybdenum stabilizes the MC carbide, reduces the molar fraction of M_7C_3 carbide and decreases the values of Fe/Cr ratio in M_7C_3 at lower temperatures. Inoue and Masumoto [3] described, inter alia, the tempering process and in-situ transformation of cementite to M_7C_3, M_7C_3 to $M_{23}C_6$, and $M_{23}C_6$ to M_6C, which occur in Fe-3.6C-17.8Cr-xMo alloys (x = 3.6 or 8, wt.%). Transformation of cementite to M_7C_3 starts approx. 600°C and it is completed at approx. 700°C. Further transformations occur at 700°C, requiring longer times of tempering.

It is known, that the wear resistance of tool and hardfacing alloys depends on the volume fraction, type and morphology of carbides, and properties of the matrix as well [25÷29].

In this study the analysis of the microstructure of the Fe-Cr-Mo-C ingot, produced in an arc furnace, is presented. Particular emphasis is placed on the determination of the morphology of eutectic, complex carbides.

2. EXPERIMENTAL

The Fe-Cr-Mo-C alloy was synthesized in an arc furnace Arc Melter AM (Edmund Bühler GmbH) in a Ti-gettered argon atmosphere. Melting of the charge was performed on a water-cooled copper mould. For further investigation the ingot, with a mass of approx. 35 g, was cut in half along the line A-A', as shown in Fig. 1.

The chemical composition was determined in the cross-section with optical emission spectrometer Foundry-Master (WAS). In order to estimate the segregation in the ingot a series of measurements on the bottom and on the cross section of the ingot were performed. Results are summarized in Table 1.

The X-Ray diffraction (XRD) analysis was performed by using a Panalytical Empyrean diffractometer using $CoK\alpha_1$ radiation (λ=1.7890 Å).

The microstructure of the alloy was examined by Nikon LV150N light microscope and FEI VERSA 3D scanning electron microscope, equipped with the energy dispersive spectroscopy (EDS) detector. Microstructure investigations were carried out on the cross-section of the ingot, after polishing and etching. The microstructure of the samples was revealed by a solution of 30 g NH_4F, 50ml HNO_3 and 20ml H_2O.

Vickers hardness measurements were performed on a TUKON 2500 hardness tester.

3. RESULTS AND DISCUSION

Table 1 shows chemical composition of the ingot, which was measured on the bottom and on the cross section of the ingot. As can be seen, the average carbon content varies significantly from 0.61 at the bottom to 0.82 (wt.%) for the cross section. It is also clear, that a segregation of molybdenum took place, as wt. % of Mo varies from 4.66 at the bottom to 5.33 for the cross section.

Table 1. Chemical composition of the ingot (wt.%).

Place of measurements	C	Si	Mn	Cr	Mo	P	S	Fe
Cross-section	0.815	0.159	0.094	24.900	5.330	0.015	0.026	Bal.
Bottom	0.613	0.206	0.100	24.600	4.660	0.100	0.014	Bal.

Figure 1 shows a photograph of the ingot and Fig. 2 the microstructure of the cross section along line A-A' (Fig. 1). During solidification on a water-cooled copper mould, three distinctive zones A, B and C were formed, indicated in Fig. 2. Dendrites in zone A, nucleated and grew in a very short time. First dendrites has an equiaxed shape (Fig. 3c). Figure 3b shows microstructure of zone B (Fig. 2), dendrites which grew parallel and opposite to the heat exchange direction, have a columnar shape. Figure 3a shows dendrites, typical for zone C (Fig. 2), formed at the end of solidification. These dendrites have similar, equiaxed shape, such as in zone A, because their latent heat is extracted radially through the undercooled melt.

XRD patterns presented in Fig. 4 show that the alloy consists of ferrite (Fe-Cr-Mo solid solution) and complex $M_{23}C_6$ carbides.

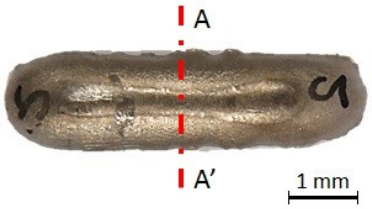

Fig. 1. A Fe-Cr-Mo-C ingot with the cross section line A-A'

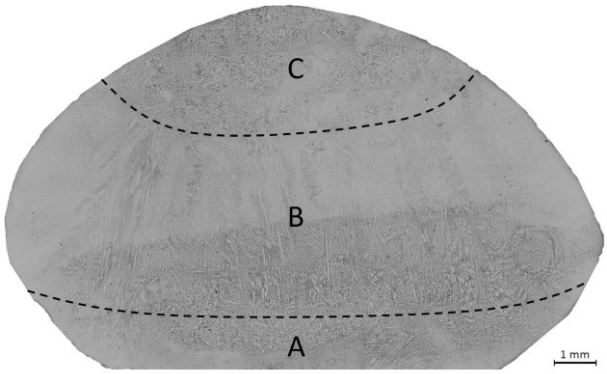

Fig. 2. The reconstructed along A-A' cross-sectional microstructure of the ingot based on images from light microscope. A – refers to inner equiaxed zone, B – refers to columnar zone, and C – refers to outer equaiaxed zone.

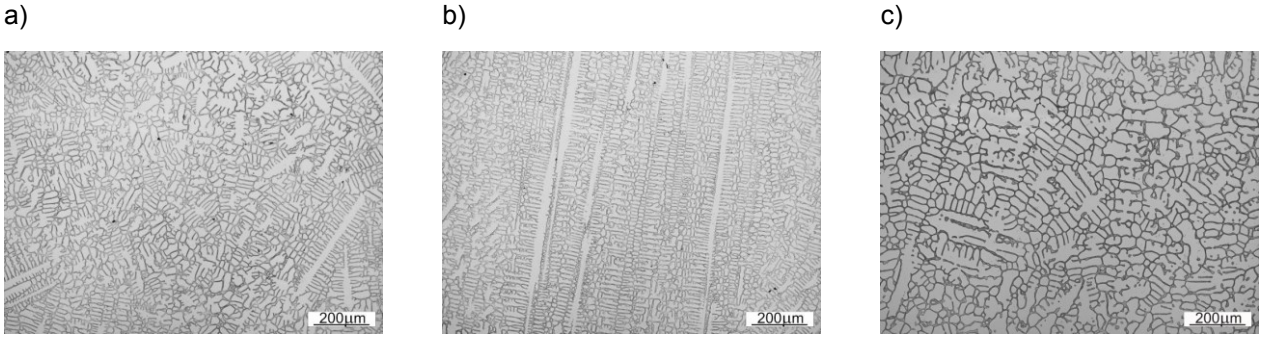

Fig. 3. Microstructure of different zones along the transverse cross-section in Fe-Cr-Mo-C ingot: a – refers to outer equaiaxed zone, b – refers to columnar zone, c – refers to inner equiaxed zone, light microscope.

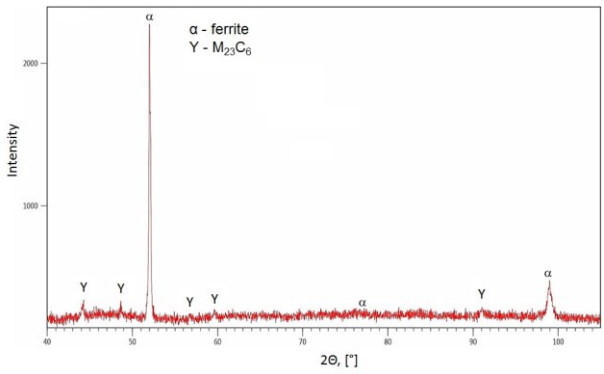

Fig. 4. XRD patterns of the investigated alloy.

Figure 5 shows the microstructure of eutectic $M_{23}C_6$ carbides observed in the aforementioned three distinctive zones. It was observed that $M_{23}C_6$ carbides formed in the interdendritic zones exhibit continuous, complex shapes. Carbides in outer and inner equiaxed zones have similar shapes. The boundary between eutectic carbides and matrix forms a continuous, longitudinal precipitation. Between the longitudinal boundaries, the carbides exhibit lamellar or polygonal character. In the columnar zone the eutectic has a longitudinal shape. Simultaneously lamellar precipitations within the eutectic boundaries make the whole a "ladder" shape.

Figure 6 shows the distribution of the major elements in dendrites and eutectic carbides. As seen, the eutectic zone is enriched in chromium and molybdenum, while the iron content is lowered.

The average hardness of the alloy is 264±5 HV10.

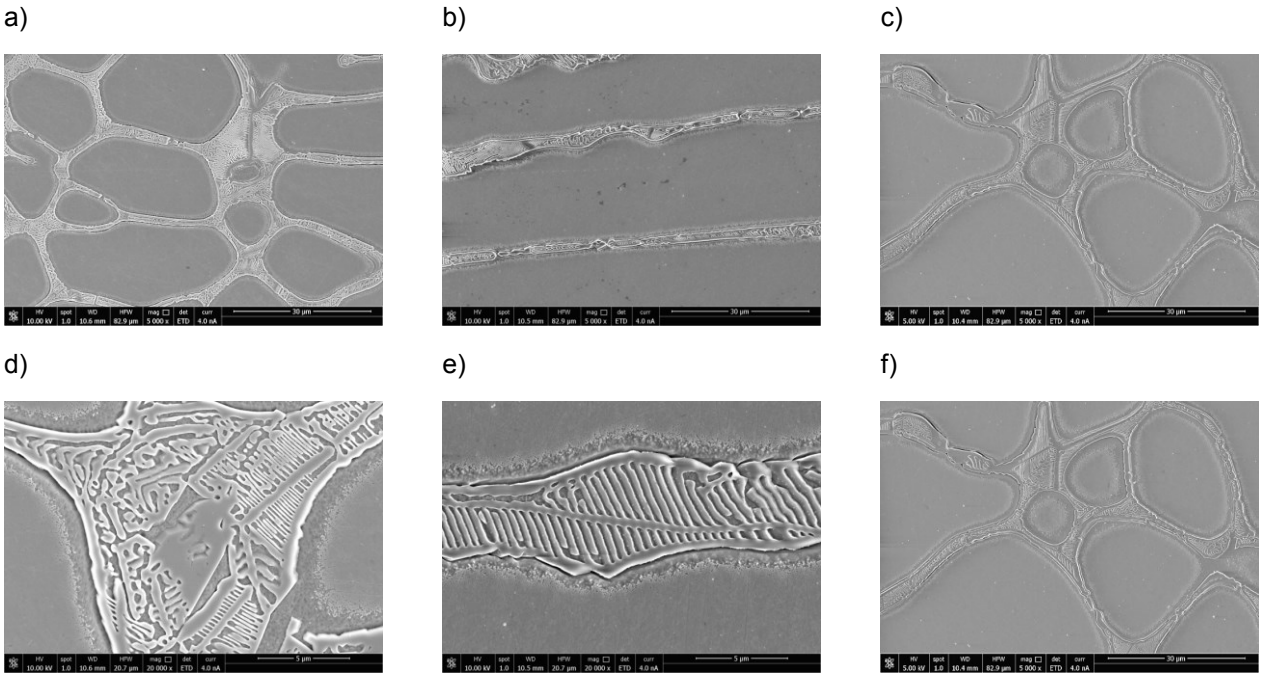

Fig. 5. Microstructure of eutectic carbides in different zones along the transverse cross-section in Fe-Cr-Mo-C ingot: a,d – refers to outer equaiaxed zone, b,e – refers to columnar zone, c,f – refers to inner equiaxed zone, SEM-SE.

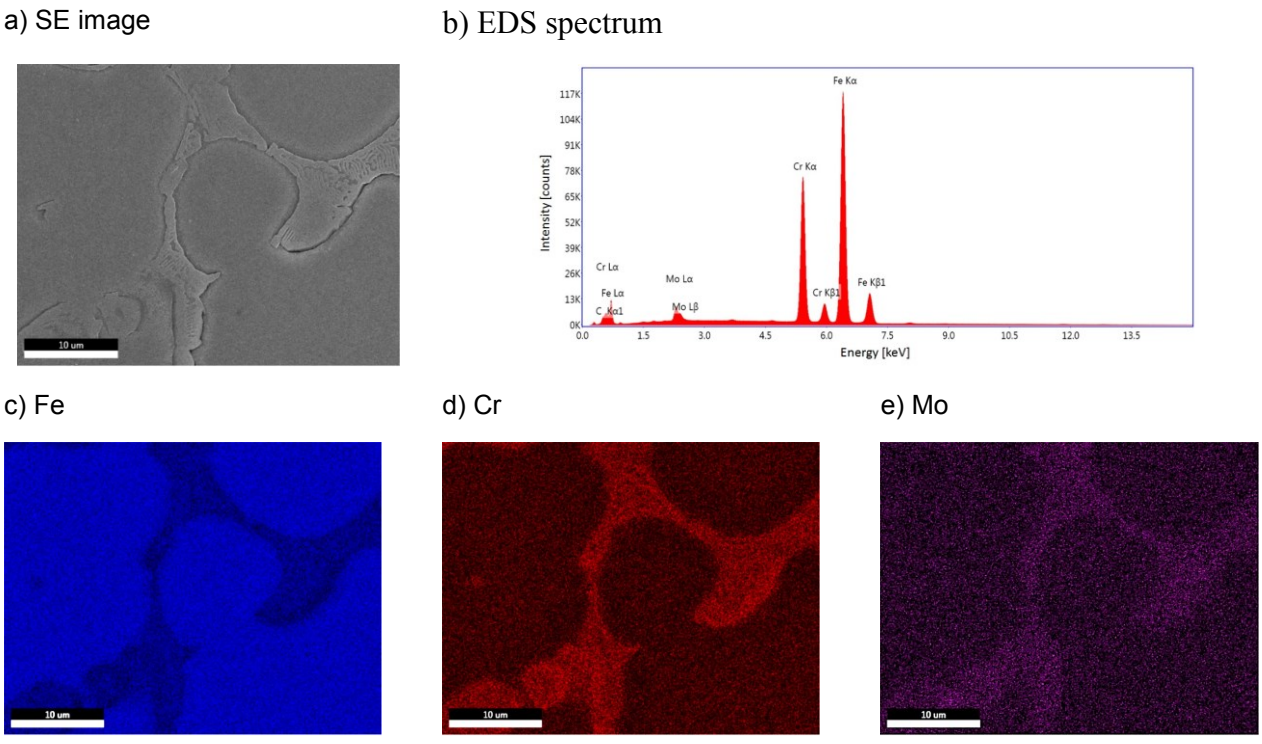

Fig. 6. X-ray mapping of element distribution in dendrite and eutectic carbides.

CONCLUSION

Fe-Cr-Mo-C alloy was synthesized and characterized in the as cast state. It consists of ferrite (Fe-Cr-Mo solid solution) and complex $M_{23}C_6$ carbides. The microstructure is composed of primary and secondary dendrites Fe-Cr-Mo solid solution with equiaxed and elongated morphology. $M_{23}C_6$ carbides formed in the interdendritic zones exhibit continuous, complex shapes. The average hardness of the alloy is 264±5 HV10.

REFERENCES

[1] M. Čekada, P. Panjan, M. Maček, P. Šmíd, Comparison of structural and chemical properties of Cr-based hard coatings, Surf. Coatings. 152 (2002) 31–35.

[2] R.G. Coltters, G.R. Belton, High Temperature Thermodynamic Properties of the Chromium Carbides Cr7C3 and Cr3C2 Determined Using a Galvanic Cell Technique, Metall. Trans. A. 14 (1983) 1915–1919.

[3] A. Inoue, T. Masumoto, Carbide reactions (M3C-M7C3-M23C6-M6C) during tempering of rapidly solidified high carbon Cr-W and Cr-Mo steels, Metall. Trans. A. 11 (1980) 739–747.

[4] M. Venkatraman, J.P. Neumann, The C-Cr (Carbon-Chromium) System, Bull. Alloy Phase Diagrams. 11 (1990) 152–159.

[5] K. Kuo, Carbide precipitation in tungsten-chromium steel below 700o, J. Iron Steel Inst. 185 (1957) 297–303.

[6] Ö.N. Doğan, J. a. Hawk, G. Laird, Solidification structure and abrasion resistance of high chromium white irons, Metall. Mater. Trans. A. 28 (1997) 1315–1328.

[7] C. Fan, M.C. Chen, C.M. Chang, W. Wu, Microstructure change caused by (Cr,Fe)23C6 carbides in high chromium Fe-Cr-C hardfacing alloys, Surf. Coatings Technol. 201 (2006) 908–912.

[8] C.M. Chang, Y.C. Chen, W. Wu, Microstructural and abrasive characteristics of high carbon Fe-Cr-C hardfacing alloy, Tribol. Int. 43 (2010) 929–934.

[9] S. Byelikov, I. Volchok, V. Netrebko, Manganese influence on chromium distribution in high-chromium cast irons, Arch. Metall. Mater. 58 (2013) 6–8.

[10] C.R. Sohar, a. Betzwar-Kotas, C. Gierl, B. Weiss, H. Danninger, Gigacycle fatigue behavior of a high chromium alloyed cold work tool steel, Int. J. Fatigue. 30 (2008) 1137–1149.

[11] P. Berthod, High temperature properties of several chromium-containing Co-based alloys reinforced by different types of MC carbides (M = Ta, Nb, Hf and/or Zr), J. Alloys Compd. 481 (2009) 746–754.

[12] P. Berthod, L. Aranda, C. Vébert, S. Michon, Experimental and thermodynamic study of the high temperature microstructure of tantalum containing nickel-based alloys, Calphad Comput. Coupling Phase Diagrams Thermochem. 28 (2004) 159–166.

[13] P. Berthod, Y. Hamini, L. Aranda, L. Héricher, Experimental and thermodynamic study of tantalum-containing iron-based alloys reinforced by carbides: Part I - Case of (Fe, Cr)-based ferritic steels, Calphad Comput. Coupling Phase Diagrams Thermochem. 31 (2007) 351–360.

[14] P. Berthod, High temperature oxidation behavior of chromium-rich alloys containing high carbides fractions. Part I: Nickel-base alloys, Mater. Corros. 64 (2013) 567–577.

[15] P. Bała, J. Pacyna, The influence of pre-tempering on the mechanical properties of HS6-5-2 high speed steel, Arch. Metall. Mater. 53 (2008) 795–801.

[16] P. Bała, Microstructural characterization of the new tool Ni-based alloy with high carbon and chromium content, Arch. Metall. Mater. 55 (2010) 1053–1059.

[17] P. Bała, Microstructure characterization of high carbon alloy from the Ni-Ta-Al-Co-Cr system, Arch. Metall. Mater. 57 (2012) 937–941.

[18] P. Bała, High Carbon Alloys from the Ni-Ta-Al-M System, AGH University of Science and Technology Press, Krakow, 2012.

[19] P. Bała, The dilatometric analysis of the high carbon alloys from Ni-Ta-Al-M system, Arch. Metall. Mater. 59 (2014).

[20] G. Cios, P. Bała, M. Stępień, K. Górecki, Microstructure of cast Ni-Cr-Al-C, Arch. Metall. Mater. 60 (2015) 145–148.

[21] H.J. Goldschmidt, Interstitial alloys, Springer Science+Business Media, LLC, New York, 1967.

[22] T. Malkiewicz, Physical metallurgy of iron alloys, Publishing House PWN, Warsaw – Cracow, 1978 (in Polish).

[23] H.M. Lee, S.M. Allen, M. Grujicic, Coarsening resistance of M2C carbides in secondary hardening steels: Part II. Alloy design aided by a thermochemical database, Metall. Trans. A. 22 (1991) 2869–2876.

[24] M. Palcut, M. Vach, R. Cicka, J. Janovec, Compositional changes in carbide M7C3 upon annealing, Arch. Metall. Mater. 53 (2008) 1157–1164.

[25] R. Chotěborský, P. Hrabě, M. Müller, J. Savková, M. Jirka, Abrasive wear of high chromium Fe-Cr-C hardfacing alloys, Res. Agric. Eng. 54 (2008) 192–198.

[26] R. Chotěborský, P. Hrabě, M. Müller, J. Savková, M. Jirka, M. Navrátilová, Effect of abrasive particle size on abrasive wear of hardfacing alloys, Res. Agric. Eng. 55 (2009) 101–113.

[27] A. Matthews, A. Leyland, K. Holmberg, H. Ronkainen, Design aspects for advanced tribological surface coatings, Surf. Coatings Technol. 100-101 (1998) 1–6.

[28] R. Dziurka, M. Madej, M. Kopyściański, M. Malyszko, M. Dziadosz, The influence of microstructure of medium carbon heat-treatable steel on its tribological properties, Key Eng. Mat. 641 (2015) 132-135.

[29] B. Łętkowska, R. Dziurka, P. Bała, The analysis of phase transformation of undercooled austenite and selected mechanical properties of low-alloy steel with boron addition, Arch. Civ. Mech. Eng. 15 (2015) 308-316.